

Tetrahedra and Physics

Frank Dodd (Tony) Smith, Jr. - viXra 1501.0078v2

Abstract

Humans perceive 3-dim Flat Space as fundamental, with a 4th-dim of Time as a necessary addition for Life to Progress. Human Mathematical study of the basic concept of the Sphere shows that 3 and 4 are very special dimensions: 3 is home of Poincare Dodecahedral Space and 4 is where Smale's Whitney trick to prove the Poincare Conjecture breaks down. 4 is also the home of Exotic R^4 .

The simplest polyhedron in 3-dim Flat Space is the Tetrahedron. The purpose of this paper is to investigate the possibility of using the Tetrahedron as a basic building block for a Realistic Theory of Physics. The Realistic Theory of Physics that I will use as a standard in this paper is my $Cl(16)$ -E8 Physics Model described in viXra 1405.0030vG.

The result of this paper is that you can combine Tetrahedra in 3-dim Flat Space but to avoid gaps in the combined structure you must curve 3-dim Space and effectively go to 4-dim Space to build 600-cell $\{3,3,5\}$ polytopes two of which can be combined to produce the 240-polytope that leads to the 8-dim Gossett polytope of the E8 Lie Algebra of $Cl(16)$ -E8 Physics whose AQFT therefore corresponds to a 4D Feynman Checkerboard Quantum Theory constructed with Tetrahedra-based structures.

If you do not curve the 3-dim space, there are two possibly useful structures:

Tetrahedral Clusters whose Periodicity corresponds to that of Real Clifford Algebras giving a correspondence with the AQFT of $Cl(16)$ -E8 Physics

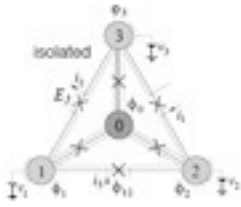
QuasiCrystals and their Approximants whose phason disorder seems to be a measure of an information deficit, and failure of equivalence, with respect to $Cl(16)$ -E8 Physics.

Table of Contents

Outline - page 2
Tetrahedral Josephson Junctions - page 5
Construction of 57G in 3-dim space - page 7
57G as Maximal Contact Grouping of cells in 600-cell - page 11
Sections of 600-cell - page 13
240 vertices of Two 600-cells and E8 - page 15
E8 Physics represented by 600-cells and 57G - page 16
Feynman Checkerboard Quantum Theory - page 22
Tetrahedra in flat space - page 35

OUTLINE:

1 - Start with a regular Tetrahedron in flat 3-dim space



Tetrahedron Josephson Junction Quantum Computer Qubit

2 - Add 4 + 12 Tetrahedra sharing faces to get 17 Tetrahedra



The 4 fit face-to-face exactly in 3-dim,

but



the 12 do not fit exactly in 3-dim,

However, all 17 do fit exactly in curved 3-dim space which is naturally embedded in 4-dim space described by Quaternions.

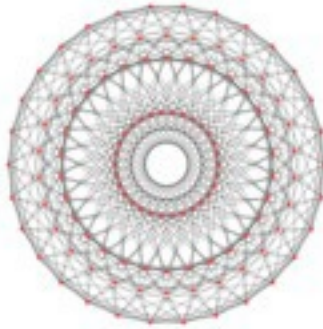
3 - Add 4 half-Icosahedra (10 Tetrahedra each) to form a 40-Tetrahedron Outer Shell around the 17 Tetrahedra and so form a 57G



Like the 12 of 17, the Outer 40 do not exactly fit together in flat 3-dim space.

If you could force all 57 Tetrahedra to fit together exactly, you would be curving 3-dim space by a Dark Energy Conformal Transformation.

4 - The 57G is the maximal contact grouping of the cells of a {3,3,5} 600-cell



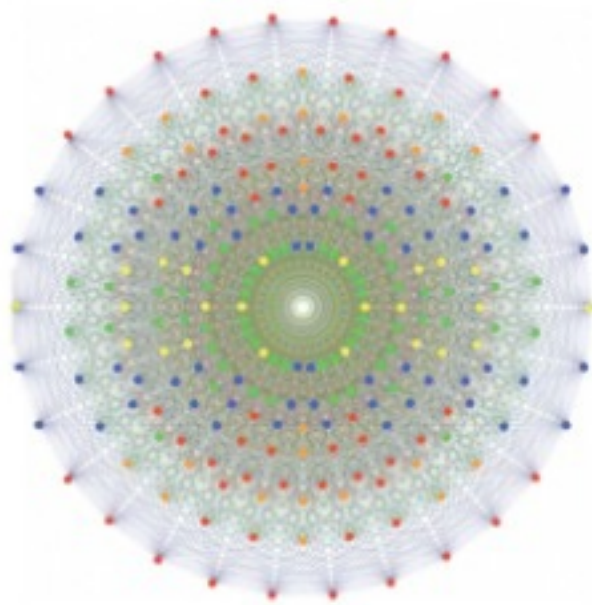
of 600 Tetrahedra and 120 vertices in 4-dim

5 - A 600-cell has 14 levels of sections beginning with a tetrahedral cell, with the top 4 sections and the bottom 4 sections each being antipodal 57G containing 57 tetrahedra and $4+4+6+12 = 26$ vertices

6 - Adding a second {3,3,5} 600-cell displaced by a Golden Ratio screw twist produces a 240 Polytope with 240 vertices in 4-dim containing four 57G as two antipodal (with respect to each 600-cell) pairs of 57G



7 - Extend 4-dim space to $4+4 = 8$ -dim space by considering the Golden Ratio algebraic part of 4-dim space as 4 independent dimensions, thus transforming the 4-dim 240 Polytope into the 240-vertex 8-dim Gosset Polytope



that represents the Root Vectors of the E8 Lie Algebra
and the first shell of an 8-dim E8 Lattice

8 - The 240 Root Vectors of 248-dimensional E8 have structure inherited from the real Clifford Algebra $Cl(16) = Cl(8) \times Cl(8)$

which structure allows construction of a E8 Physics Lagrangian from which realistic values of particle masses, force strengths, etc., can be calculated.

Tetrahedra can be used as Josephson Junctions.

A very useful reference is the 2003 dissertation of Christopher Bell at St. John's College Cambridge entitled "Nanoscale Josephson devices", on the web at http://www.dspace.cam.ac.uk/bitstream/1810/34607/1/chris_bell_thesis.pdf

Feigelman, Ioffe, Geshkenbein, Dayal, and Blatter in cond-mat/0407663 say: "... Superconducting tetrahedral quantum bits ...

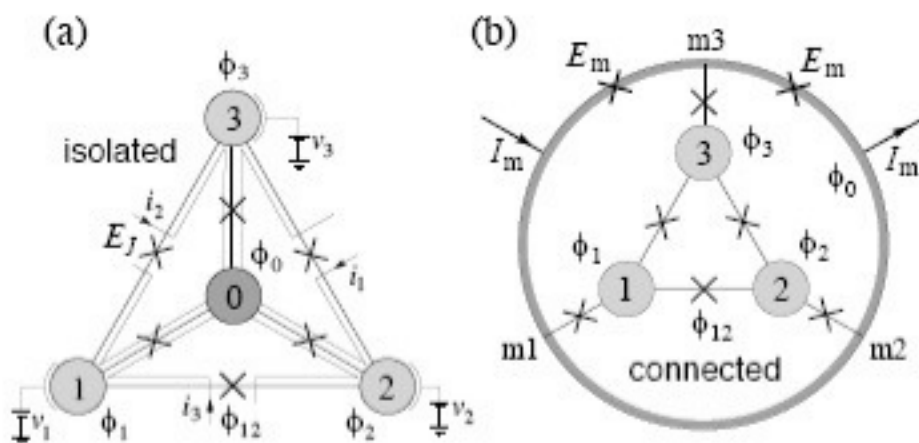


FIG. 1: (a) Tetrahedral superconducting qubit involving four islands and six junctions (with Josephson coupling E_J and charging energy E_C); all islands and junctions are assumed to be equal and arranged in a symmetric way. The islands are attributed phases ϕ_i , $i = 0, \dots, 3$. The qubit is manipulated via bias voltages v_i and bias currents i_i . In order to measure the qubit's state it is convenient to invert the tetrahedron as shown in (b) — we refer to this version as the 'connected' tetrahedron with the inner dark-grey island in (a) transformed into the outer ring in (b). The measurement involves additional measurement junctions with couplings $E_m \gg E_J$ on the outer ring which are driven by external currents I_m (schematic, see Fig. 6 for details); the large coupling E_m effectively binds the ring segments into one island.

... The novel tetrahedral qubit design we propose below operates in the phase-dominated regime and exhibits two remarkable physical properties:

first, its non-Abelian symmetry group (the tetrahedral group T_d) leads to the natural appearance of degenerate states and appropriate tuning of parameters provides us with a doubly degenerate groundstate. Our tetrahedral qubit then emulates a spin-1/2 system in a vanishing magnetic field, the ideal starting point for the construction of a qubit.

Manipulation of the tetrahedral qubit through external bias signals translates into application of magnetic fields on the spin; the application of the bias to different elements of the tetrahedral qubit corresponds to rotated operations in spin space.

Furthermore, geometric quantum computation via Berry phases ... might be implemented through adiabatic change of external variables.

Going one step further, one may hope to make use of this type of systems in the future physical realization of non-Abelian anyons, thereby aiming at a new generation of topological devices ... which keep their protection even during operation ...

The second property we wish to exploit is geometric frustration:

In our tetrahedral qubit ... it appears in an extreme way by rendering the classical minimal states continuously degenerate along a line in parameter space. Semi-classical states then appear only through a fluctuation-induced potential, reminiscent of the Casimir effect ... and the concept of inducing 'order from disorder' ...

The quantum-tunneling between these semi-classical states defines the operational energy scale of the qubit, which turns out to be unusually large due to the weakness of the fluctuation-induced potential. Hence the geometric frustration present in our tetrahedral qubit provides a natural boost for the quantum fluctuations without the stringent requirements on the smallness of the junction capacitances, thus avoiding the disadvantages of both the charge- and the phase- device:

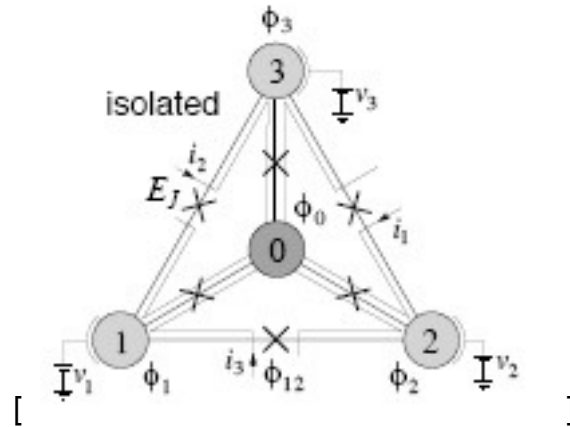
The larger junctions reduce the demands on the fabrication process and the susceptibility to charge noise and mesoscopic effects, while the large operational energy scale due to the soft fluctuation-induced potential reduces the effects of flux noise. Both types of electromagnetic noise, charge- and flux noise, appear only in second order ...

in order to benefit from a protected degenerate ground state doublet, the qubit design requires a certain minimal complexity; it seems to us that the tetrahedron exhibits the minimal symmetry requirements necessary for this type of protection and thus the minimal complexity necessary for its implementation. ...”.

Construction of 57G in 3-dim space

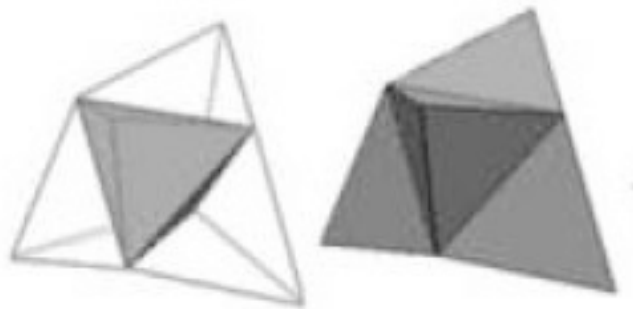
Eric A. Lord, Alan L. Mackay, and S. Ranganathan in their book “New Geometries for New Materials” (Cambridge 2006) said:

“... The gamma-Brass cluster ... starts from a single tetrahedron



Place four spheres in contact.

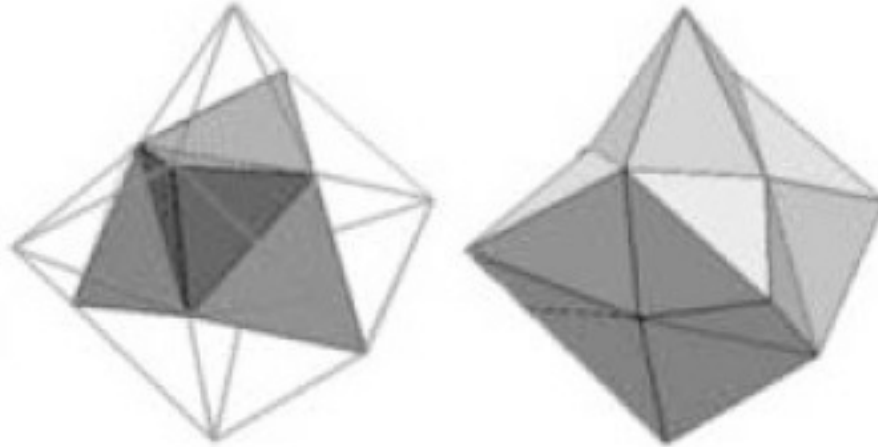
Then place a sphere over each face of the tetrahedral cluster.
The centres and bonds then form a stella quadrangula



built from five regular tetrahedra ...[a total of $1+4 = 5$ tetrahedra]...

Six more spheres [vertices] placed over the edges of the original tetrahedron form an octagonal shell. In terms of the network of centres and bonds we now have added 12 [= 2×6] more tetrahedra ...

There are now five tetrahedra around each edge of the original tetrahedron. ...



...[we now have $1+4+12 = 17$ tetrahedra]...

[The 12 newly added tetrahedra]... are not quite regular ...[i.e., nonzero Fuller unzipping angles appear as described by Thomas Banchoff in his book “Beyond the Third Dimension” (Scientific American Library 1990) where he said:

“... in three-space we can fit five tetrahedra around an edge ...

[image from Conway and Torquato PNAS 103 (2006) 10612-10617

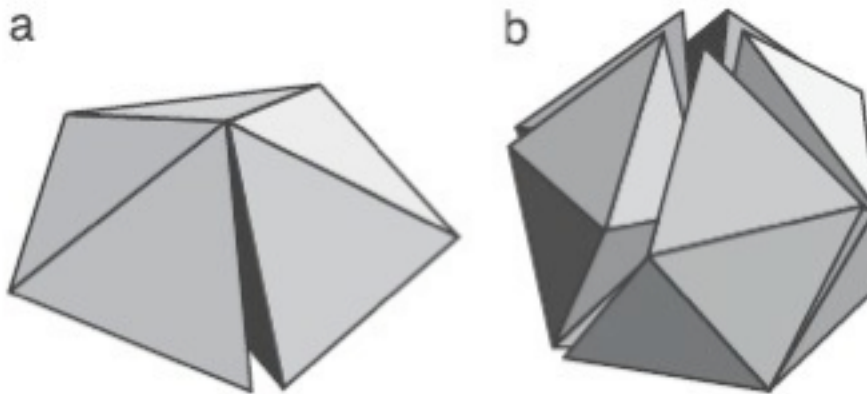


Fig. 1. Certain arrangements of tetrahedra. (a) Five regular tetrahedra about a shared edge. The angle of the gap is 7.36° . (b) Twenty regular tetrahedra about a shared vertex. The gaps amount to 1.54 steradians.]

... with a ... small amount of room to spare, which allows folding into 4-space ...[where the fit can be made exact]...”.

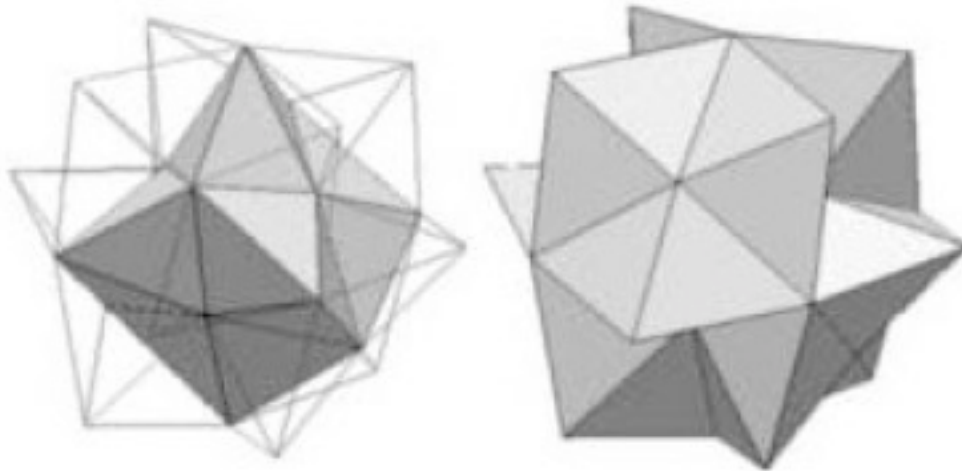
Note that all the subsequently added tetrahedra of layers and structures further out from the center are also “not quite regular”, or, in other words, leave gaps among tetrahedra that are related to the Fuller unzipping angle.

The irregularity, or Fuller unzipping angle, can be visualized as the amount of curvature in a collection of tetrahedra by which it deviates from the flatness of 3-dim space described by the 3-dim Diamond Lattice.

The irregularity goes away in curved 3-dim space, which, if it is to be realized in a flat space, must be realized in 4-dim space by adding a 4th dimension to 3-dim space.

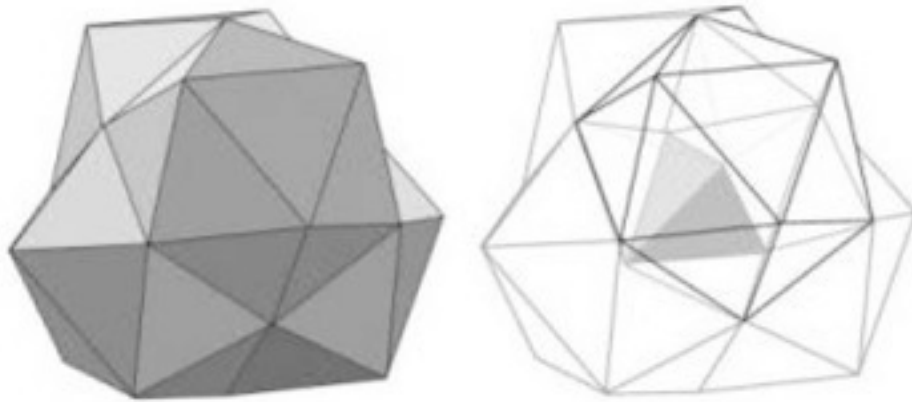
However, for now, we will continue with construction of the 57G and its Array in 3-dim space, and leave additional dimensions to later sections of this paper.]

... 12 more spheres [vertices in addition to the $1+4+12 = 17$] complete the rings of five tetrahedra around the edges of the four secondary tetrahedra ...[They add $2 \times 12 = 24$ more tetrahedra for a total of $1+4+12+24 = 41$ tetrahedra]...



... Without increasing the number of vertices [which is now 26],

inserting 16 more tetrahedra reveals the structure to be four interpenetrating icosahedra sharing a common tetrahedral building block ...



...[and gives a total of $41 + 16 = 57$ tetrahedra]... and 26 vertices ... the model of the 26-atom gamma-brass cluster as four interpenetrating icosahedral clusters ...".

Note that each of the 4 interpenetrating icosahedra has:

- 10 tetrahedra to itself (each belongs to only 1)
- 6 tetrahedra shared with one other (each belongs to 2)
- 3 tetrahedra shared with two others (each belongs to 3)
- 1 tetrahedron shared with all three others (belongs to 4)

so

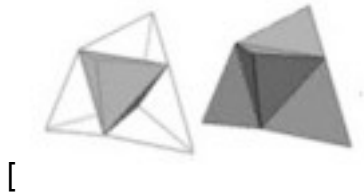
the total number of tetrahedra in a 57G
is $4 \times 10 + 4 \times 6/2 + 4 \times 3/3 + 4 \times 1/4 = 40 + 12 + 4 + 1 = 57$.

57G as Maximal Contact Grouping of cells in 600-cell

The Wikipedia entry on the 600-cell says:

“... the 600-cell ... is the convex regular polytope ... $\{3,3,5\}$. Its boundary is composed of 600 tetrahedral cells with 20 meeting at each vertex ... they form 1200 triangular faces, 720 edges, and 120 vertices. The edges form 72 flat regular decagons. Each vertex of the 600-cell is a vertex of six such decagons. ... Its vertex figure is an icosahedron ... It has a dihedral angle of 164.48 degrees. ... Each cell touches, in some manner, 56 other cells.

[$4+1 = 5$] One cell contacts each of the four faces;



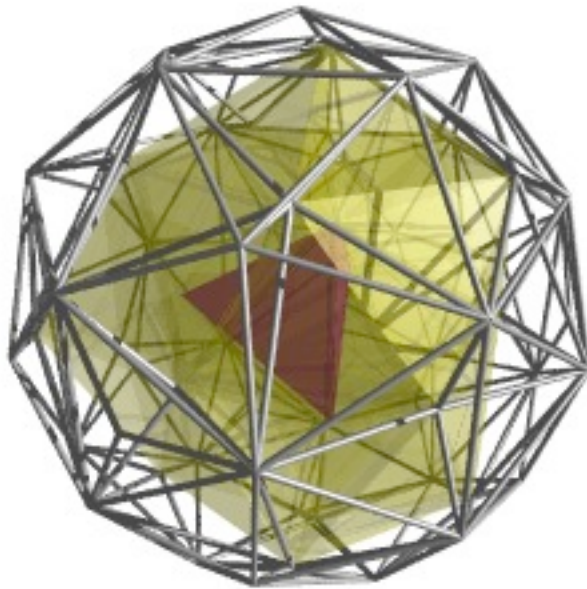
[$2 \times 6 + 5 = 17$] two cells contact each of the six edges, but not a face;



[$10 \times 4 + 17 = 57$] and ten cells contact each of the four vertices, but not a face or edge.



This image shows the 600-cell in cell-first perspective projection into 3D. ...



... The nearest cell to the 4d viewpoint is rendered in solid color, lying at the center of the projection image.

The cells surrounding it (sharing at least 1 vertex) are rendered in transparent yellow.
[**They are a 57G Maximal Contact Grouping**]

The remaining cells are rendered in edge-outline.
Cells facing away from the 4D viewpoint have been culled for clarity. ...”.

Sections of 600-cell

Sadoc and Mosseri in their book “Geometrical Frustration” (Cambridge 1999, 2006), say: “...

250

A5 Polytope {3, 3, 5}

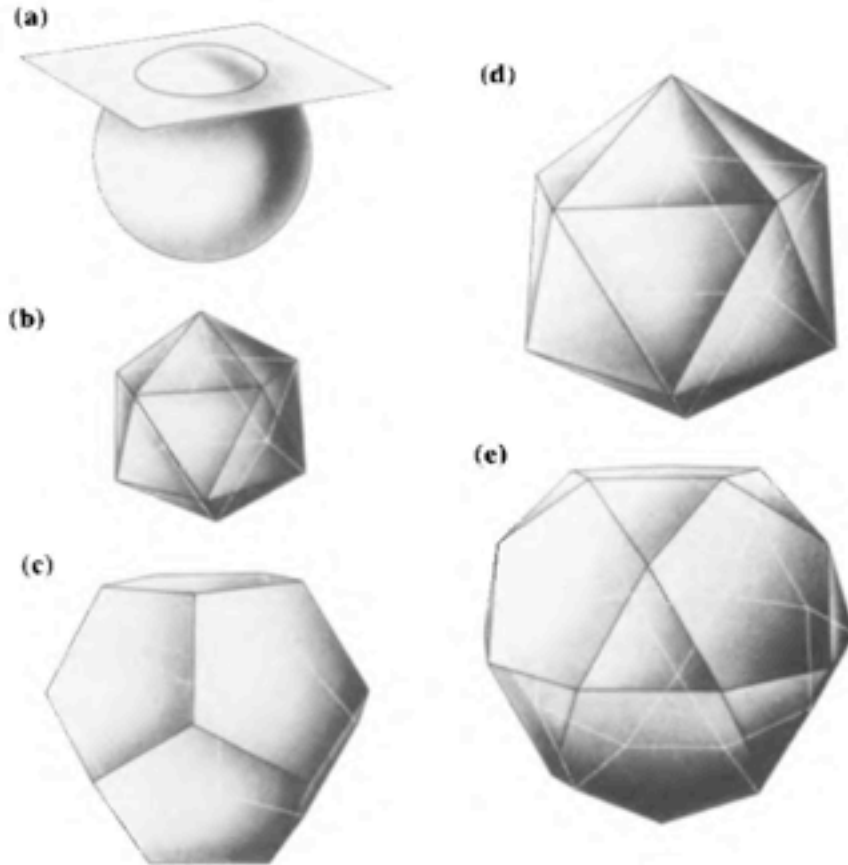


Fig. A5.1. The $\{3, 3, 5\}$ polytope. Different flat sections in S^3 (with one site on top) give the following successive shells; (a) an icosahedral shell formed by the first 12 neighbours, (b) a dodecahedral shell, (c) a second and larger icosahedral shell, (d) an icosidodecahedral shell on the equatorial sphere. Then other shells are symmetrically disposed in the second ‘south’ hemi-hypersphere, relative to the equatorial sphere (e).

$\omega = \pi/2$: the ‘equatorial’ sphere is tiled by 30 vertices which form a regular icosidodecahedron. For larger values of ω , the situation is then symmetrical with respect to the equatorial sphere.

$\omega = 3\pi/5$: an icosahedron.

$\omega = 2\pi/3$: a dodecahedron.

$\omega = 4\pi/5$: an icosahedron.

$\omega = \pi$: one vertex at the south pole $x_0 = -R, x_1 = x_2 = x_3 = 0$.

...

Table A5.1. Sections of the $\{3, 3, 5\}$ polytope (with an edge length equal to $2\tau^{-1}$) beginning with a vertex

Section	x_0	$(x_1, x_2, x_3)^{\dagger}$	Vertex number	Shape
0	2	(0, 0, 0)	1	point
1	τ	(1, 0, τ^{-1})	12	icosahedron
2	1	(1, 1, 1)	20	dodecahedron
		($\tau, \tau^{-1}, 0$)		
3	τ^{-1}	($\tau, 0, 1$)	12	icosahedron
4	0	(2, 0, 0)	30	icosidodecahedron
		($\tau, 1, \tau^{-1}$)		
5	$-\tau^{-1}$	($\tau, 0, 1$)	12	icosahedron
6	-1	(1, 1, 1)	20	dodecahedron
		($\tau, \tau^{-1}, 0$)		
7	$-\tau$	(1, 0, τ^{-1})	12	icosahedron
8	-2	(0, 0, 0)	1	point

[†]Cyclic permutation with all possible changes of signs. $\tau = (1 + \sqrt{5})/2$.

... Another ... description consists of fixing a polytope cell center at the north pole ...

Table A5.2. Section of the $\{3, 3, 5\}$ polytope (edge length $2\tau^{-1}\sqrt{2}$) beginning with a cell

Section	x_0	(x_1, x_2, x_3)	Vertex number	Shape
0	τ^2	($\tau^{-1}, \tau - 1, \tau^{-1}$) [†]	4	tetrahedron
1	$\sqrt{5}$	(-1, 1, 1)	4	tetrahedron
2	2	(2, 0, 0)	6	octahedron
3	τ	(τ, τ, τ^{-2})	12	distorted
4	1	($\sqrt{5}, 1, 1$)	12	cubo-octahedron
5	τ^{-1}	($\tau^2, \tau^{-1}, \tau^{-1}$)	12	
6	τ^{-2}	(τ, τ, τ)	4	tetrahedron
7	0	(2, 2, 0)	12	cubo-octahedron
8	$-\tau^{-2}$	($-\tau, \tau, \tau$)	4	tetrahedron
—	—	—	—	—
14	$-\tau^2$	($-\tau^{-1}, \tau^{-1}, \tau^{-1}$)	4	tetrahedron

[†]Permutation with an even number of sign changes. $\tau = (1 + \sqrt{5})/2$. Distorted cubo-octahedra are such that their square faces are changed into golden rectangles.

... ". At the north pole and its antipodal south pole are
Maximal Contact Groupings (57G) with 4+4+6+12 = 26 vertices.

240 vertices of Two 600-cells and E8

Sadoc and Mosseri in that book also say:

“... $\{3,3,5\}$ vertices ... as a set of 120 unit quaternions, form the binary icosahedral group ... the 120 polytope vertices can be grouped into four symmetry related sets of 30 sites, whose local order is linear arrangement of tetrahedra resembling Coxeter’s



‘simplicial helix’ ...

... In R^3 , the simplicial helix has

pseudo-periods ... every 30 tetrahedra, the structure almost repeats itself ... In the polytope ... $\{3,3,5\}$... the set of 30 tetrahedra perfectly closes on itself on a great circle

...

It is possible to describe the $\{3,3,5\}$ polytope using the ... spherical torus which is a two-dimensional surface embedded in the spherical space S^3 ... [that] ... can be built from a square sheet, whose opposite sides are joined together. ...

Any line parallel to a diagonal of the square corresponds to a great circle of the 3-sphere ... For the spherical torus ... the two ‘axes’ of the torus ... are great circles ... the $\{3,3,5\}$ polytope has two sets of 10 vertices ... on the two opposite axes of the torus foliation. The remaining 100 vertices belong to two sets of 50 vertices, forming triangular tilings on two tori ... placed symmetrically ... to the spherical torus.



We can represent one such torus by a cylinder ...

...

if we decompose further the sets of 50 vertices on each torus into five sets of 10 vertices, we ... get ... 12 sets of 10 vertices belonging to 12 great circles, which is .. the discretized Hopf fibration ... The Hopf mapping of this discrete set onto S^2 gives 12 points which form a regular icosahedron on the base

...

The E_8 lattice is ... the densest sphere packing in eight dimensions ...

[its] first ... shell is a 240-vertex ... Gosset polytope ...

split its 240 vertices into ten ... subsets ... each ... belonging ... to a sphere S^3 ...

This is ... a discrete version of the Hopf fibration of S^7 with S^3 fibres and a S^4 base

...

On each fibre, the 24 points form a [24-cell] polytope $\{3,4,3\}$...

each fibre ... generates a four-dimensional sublattice $\{3,3,4,3\}$ of the E_8 lattice.

There are ten ... sublattices through the origin, associated with the ten points on the base S^4 ... a ‘cross’ polytope on S^4 ... images of the fibres under the Hopf map.

Let P be ... $(1/\sqrt{5})(1,1,1,1,1)$... It ... defines a four-dimensional space E .

The mapping of the Gosset polytope onto E produces two sets of five $(3,4,3)$...

form[ing] ... two concentric $\{3,3,5\}$ on E ... which differ by a factor [of the Golden Ratio]

...”

E8 Physics represented by 600-cells and 57G

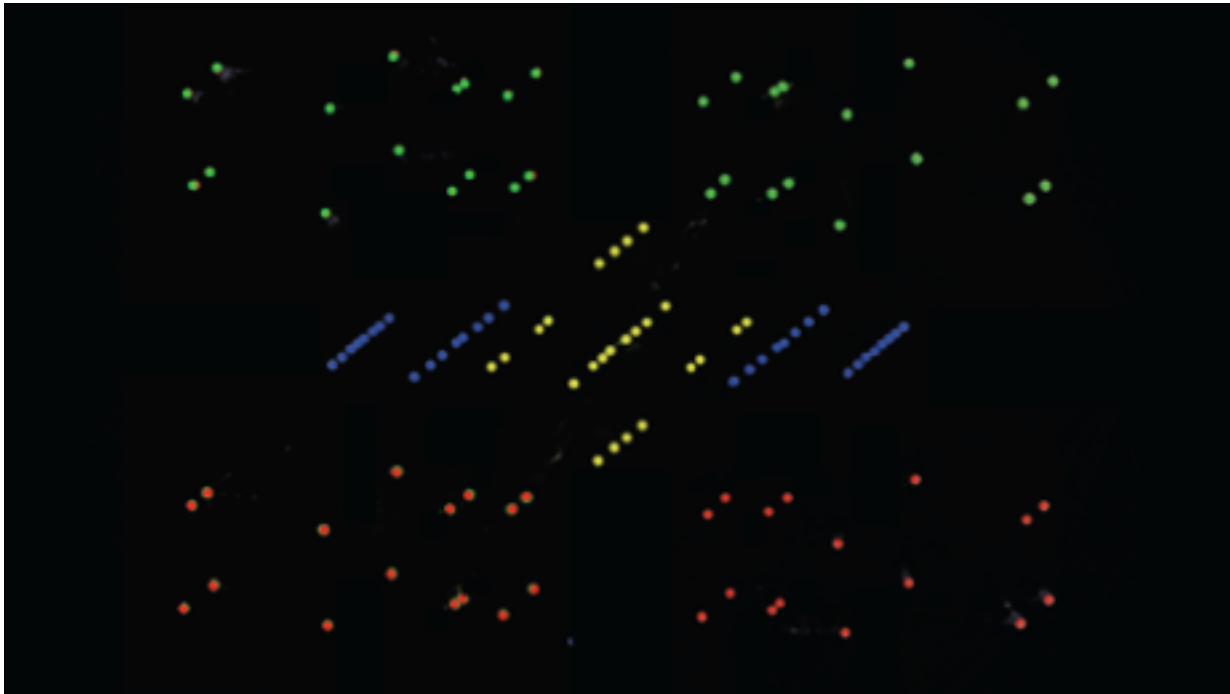
E8 Physics is described in <http://vixra.org/pdf/1405.0030vG.pdf> in which the 240 vertices of the Gosset polytope are given physical interpretations that produce a Local Classical Lagrangian for Gravity and the Standard Model. Embedding E8 in the Real Clifford Algebra $Cl(16) = Cl(8) \times Cl(8)$ and taking the completion of the union of all tensor products of $Cl(16)$ gives a realistic Algebraic Quantum Field Theory (AQFT).

An equivalent Quantum Field Theory can be constructed using Tetrahedra, 57G, 600-cells, and the E8 Gossett polytope along with a generalized Feynman Checkerboard in 4 SpaceTime dimensions.

To begin, consider the two 600-cells underlying the Gosset polytope at each vertex of an E8 Lattice.

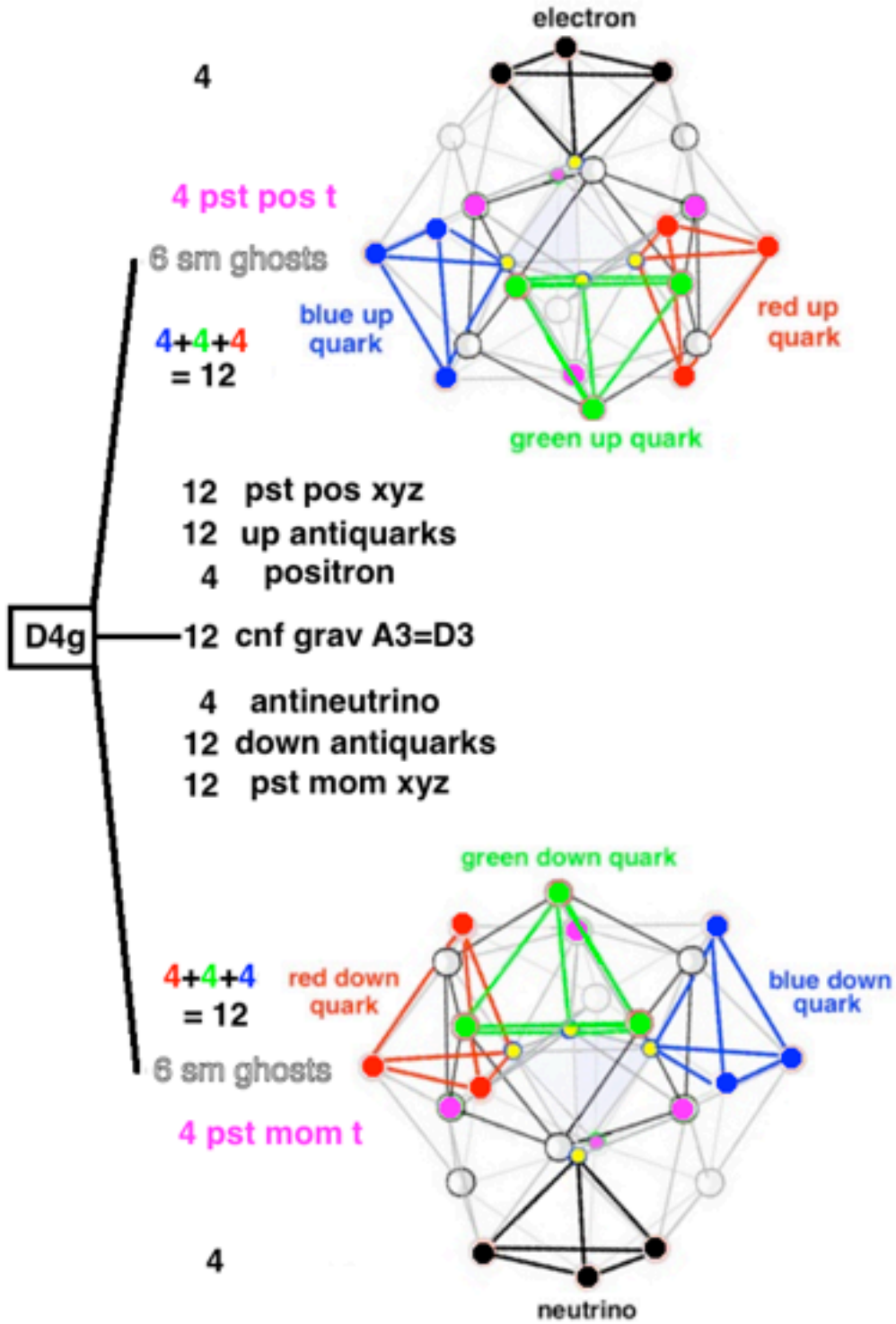
Split 8-dim Kaluza-Klein E8 SpaceTime into its two 4-dimensional components: M4 Physical SpaceTime and $CP^2 = SU(3 / SU(2) \times U(1)$ Internal Symmetry Space

Let one 600-cell represent Gravity and physics of Physical SpaceTime. Here is a projection of its 120 vertices whose physical interpretations are:
red and green = Components of Fermions, blue = M4 Physical SpaceTime, yellow = D4g of Conformal Gravity and Standard Model Ghosts

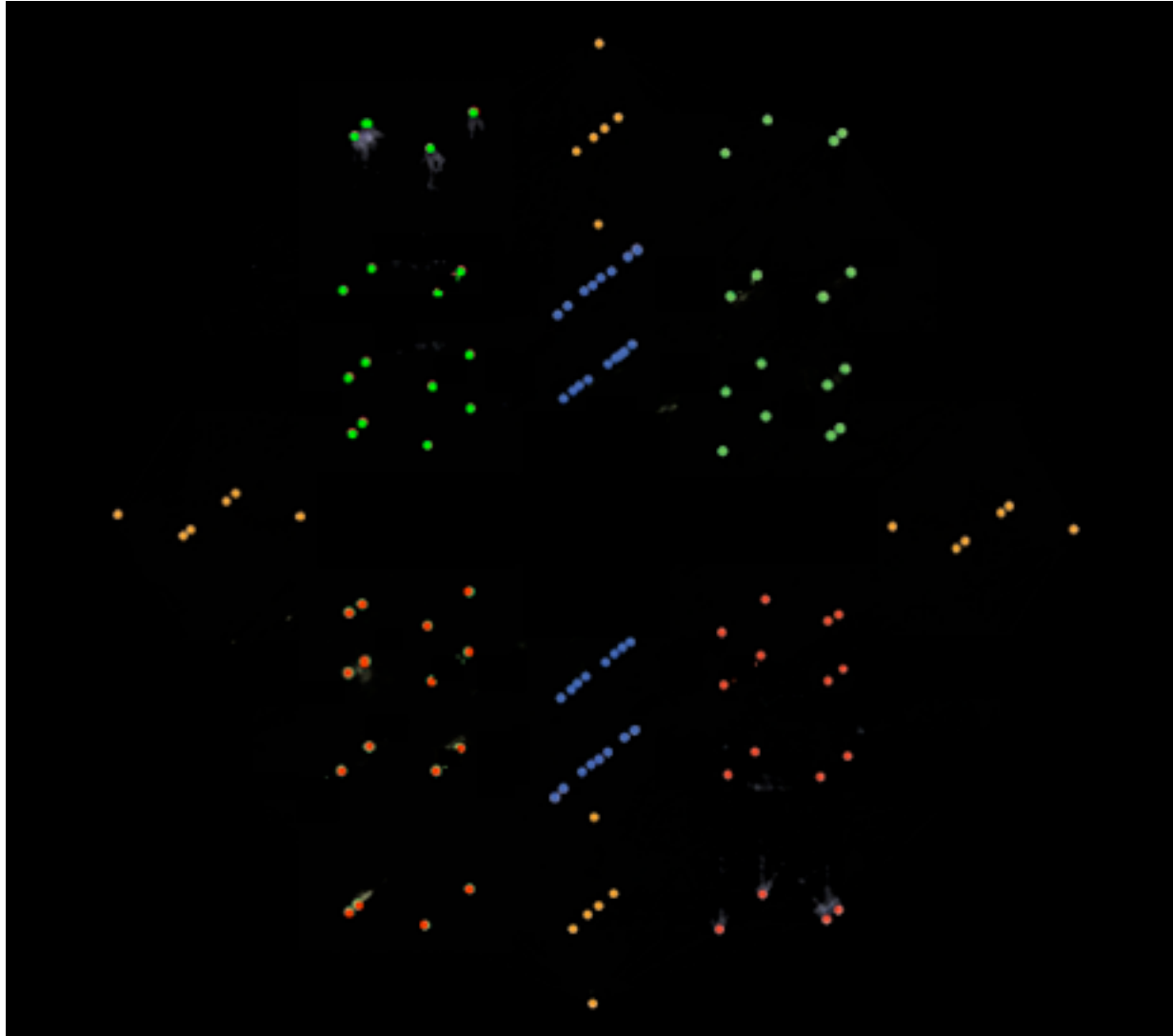


Here is how those 120 vertices appear in cell-centered sections of the D4g 600-cell:

Conformal Gravity 600-Cell with M4 Physical SpaceTime

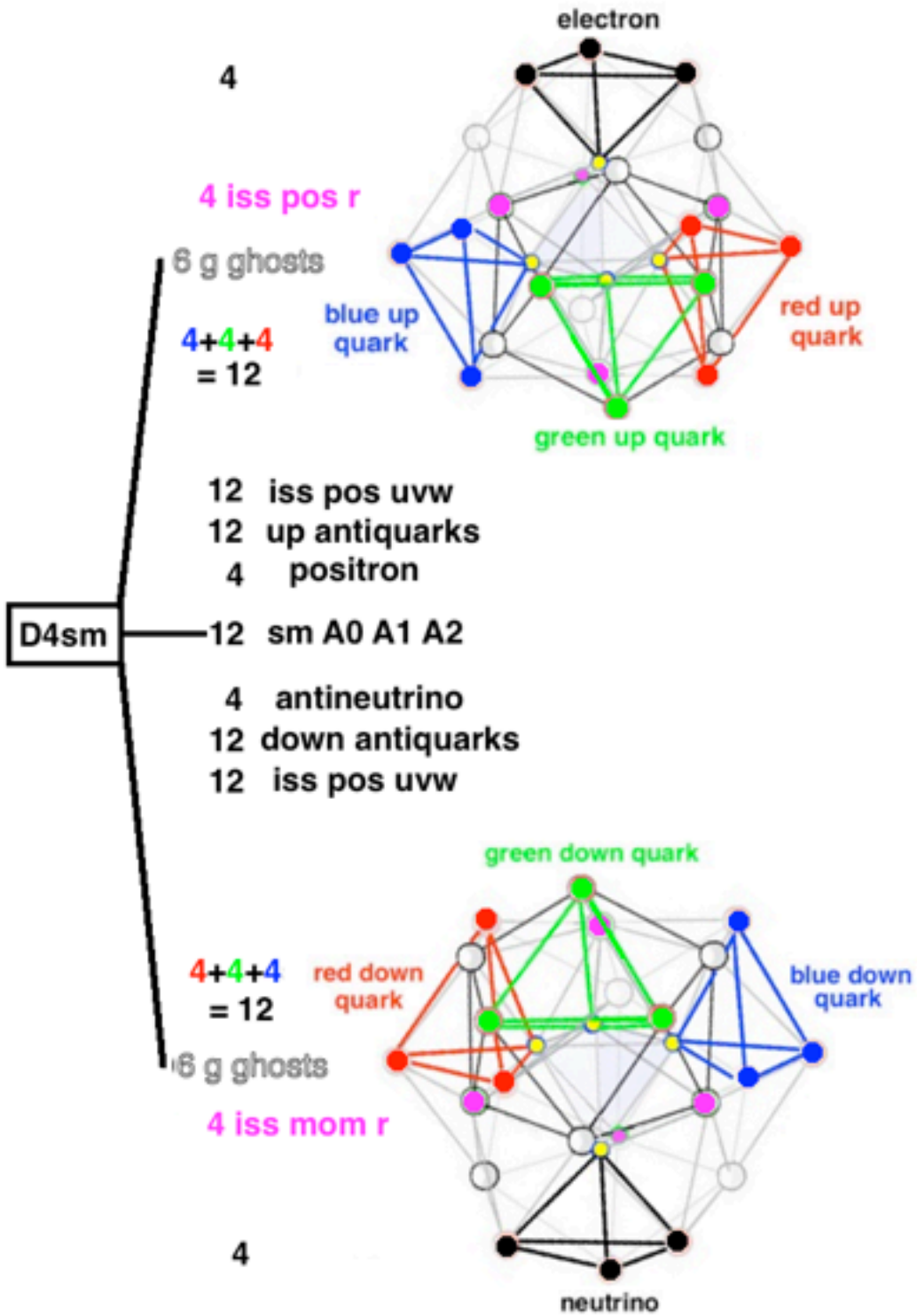


Let the other 600-cell represent the Standard Model and its Internal Symmetry Space.
Here is a projection of its 120 vertices whose physical interpretations are:
red and green = Components of Fermions, blue = CP2 Internal Symmetry Space,
orange = D4sm of the Standard Model and Conformal Gravity Ghosts

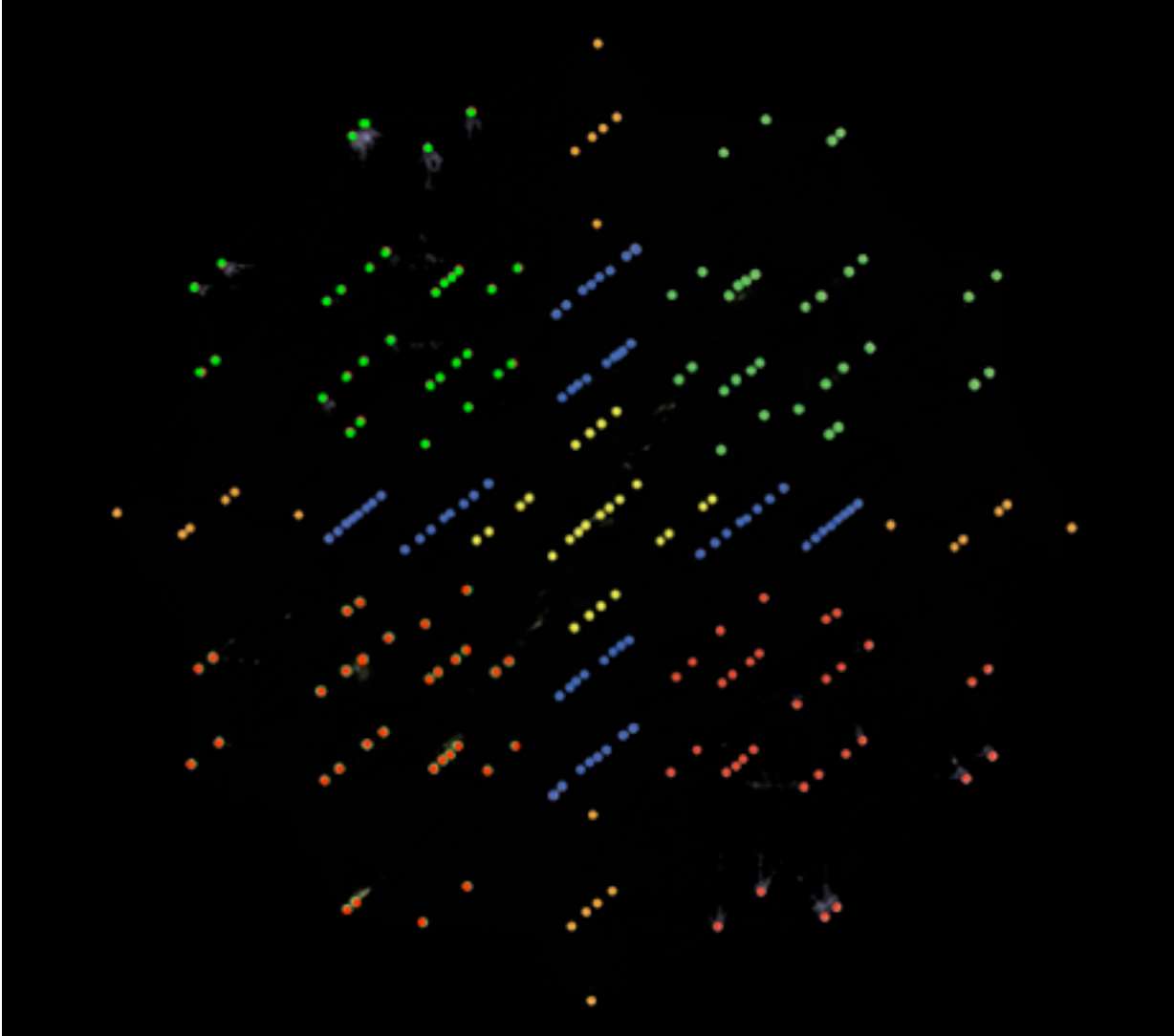


Here is how those 120 vertices appear in cell-centered sections of the D4sm 600-cell:

Standard Model 600-Cell with CP2 Internal Symmetry Space

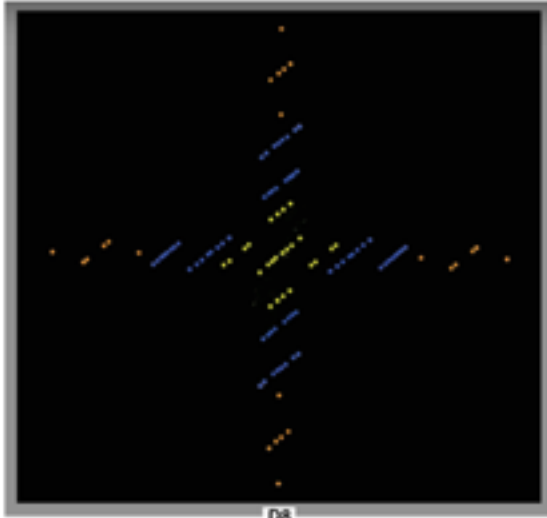


The 120 vertices of the D4g 600-cell and the 120 vertices of the D4sm 600-cell combined form the 240 vertices of the E8 Root Vectors of E8 Physics:

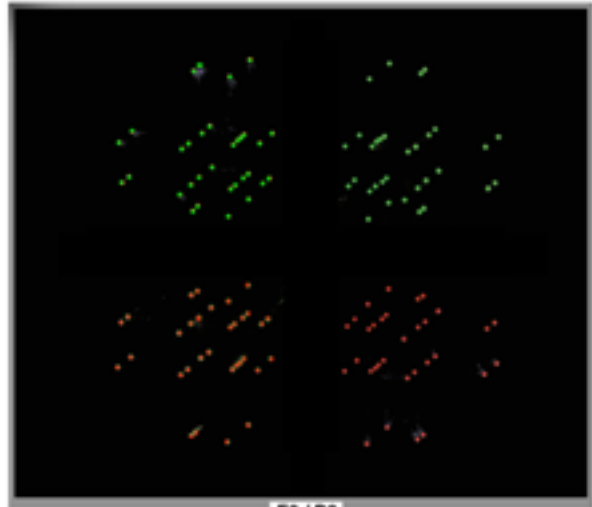


E8 lives inside the Real Clifford Algebra $Cl(16)$ as $E8 = D8 + Cl(16)$ half-spinors
so

240 E8 Root Vectors = 112 D8 Root Vectors + 128 $Cl(16)$ half-spinors



D8



E8 / D8

$E8$ Lattice = $D8$ Lattice + ($[1] + D8$ Lattice)
where the lattice shifting glue vector $[1] = (1/2, \dots, 1/2)$

Since all the E8 lattices have in common the vertices $\{ \pm 1, \pm i, \pm j, \pm k, \pm e, \pm ie, \pm je, \pm ke \}$, all the charged Dirac fermions can interact with each other. Composite particles, such as Quark-AntiQuark mesons and 3-Quark hadrons, propagate on the common parts of the E8 lattices involved. The uncharged neutrino fermion, which corresponds to the Octonion real axis with basis $\{1\}$, propagates on the 8th Kirmse E8 Lattice that is not an independent Octonion Integral Domain.

If a preferred Quaternionic Structure is introduced into an Octonionic E8 Lattice then the Octonionic E8 Lattice is transformed into Quaternionic Lattice structure. The Quaternionic Integral Domain Lattice is the D4 Lattice.

D8 Lattice is transformed to $D4g + D4sm$

$([1] + D8 \text{ Lattice})$ is transformed to $([1] + D4g) + ([1] + D4sm)$

so

E8 is transformed to $\{ D4g + ([1] + D4g) \} + \{ D4 sm + ([1] + D4sm) \}$

$$\mathbf{E8 = D+4g + D+4sm}$$

D+4g corresponds to the 600-cell containing D4g

D+4sm corresponds to the 600-cell containing D4sm

Conway and Sloane (Sphere Packings, Lattices, and Groups - Springer) (Chapter 4, eq. 49)

give equations for the number of vertices $N(m)$ in the m -th layer

of the $D+4$ HyperDiamond lattice where d is a divisor (including 1 and m) of m :

for m odd: $N(m) = 8 \text{ SUM}(d|m) d$ for m even: $N(m) = 24 \text{ SUM}(d|m, d \text{ odd}) d$

Here are the numbers of vertices in some of the layers of the $D4+$ lattice.

The even-numbered layers correspond to the even $D4$ sublattice:

m =norm of layer	$N(m)$ =no. vert.
0	1
1	8 = 1 x 8
2	24 = 1 x 24
3	32 = (1 + 3) x 8
4	24 = 1 x 24
5	48 = (1 + 5) x 8
6	96 = (1 + 3) x 24
7	64 = (1 + 7) x 8
8	24 = 1 x 24
9	104 = (1 + 3 + 9) x 8
10	144 = (1 + 5) x 24
11	96 = (1 + 11) x 8
12	96 = (1 + 3) x 24
13	112 = (1 + 13) x 8
14	192 = (1 + 7) x 24
15	192 = (1 + 3 + 5 + 15) x 8
16	24 = 1 x 24
17	144 = (1 + 17) x 8

First Stage of 4D Feynman Checkerboard:

$D+4g$ vertices have HyperOctahedron 8 nearest-neighbors $\{+/-1, +/-i, +/-j, +/-k\}$

where 4-dim $1, i, j, k$ are descendants of 8-dim $1, i, j, k$

to be used as 4D Feynman Checkerboard Primary Links representing the 4-dim $M4$ Physical SpaceTime of the Kaluza-Klein of $E8$ Physics whose 4 basis elements are $\{1, i, j, k\}$ each of which has 8 momentum components with respect to 8-dim SpaceTime to represent $4 \times 8 = 32$ of 600-cell vertices.

$D+4g$ vertices have 24-cell 24 next-nearest neighbors representing the 12 Conformal Gravitons (Root Vectors of $U(2,2)$ and 12 Ghosts of Standard Model Gauge Bosons that live on the nearest-neighbor links and represent 24 of 600-cell vertices.

$D+4g$ vertices have 6-semi-HyperCube 32 next-next-nearest neighbors representing 4 $M4$ Physical SpaceTime components of 8 First-Generation Fermion Particles. Fermion AntiParticles are represented by Particles moving backward in Time for representation of $2 \times 32 = 64$ of 600-cell vertices.

$D+4g$ odd (1 and 3) layers correspond to Vectors and Fermion Spinors which are related by Triality.
 $D+4g$ even (2) layers correspond to BiVectors.

From each vertex of the 4D Feynman Checkerboard the First Stage uses a Triad of Quantum Choice Vectors.

Second Stage of 4D Feynman Checkerboard:

D+4sm vertices have HyperOctahedron 8 nearest-neighbors $\{+/-1, +/-i, +/-j, +/-k\}$
where 4-dim $1, i, j, k$ are descendants of 8-dim E, I, J, K
to be used as 4D Feynman Checkerboard Secondary Links representing the
4-dim CP2 Internal Symmetry Space of the Kaluza-Klein of E8 Physics whose
4 basis elements are $\{1, i, j, k\}$ each of which has 8 momentum components
with respect to 8-dim SpaceTime to represent $4 \times 8 = 32$ of 600-cell vertices.

D+4sm vertices have 24-cell 24 next-nearest neighbors representing the
12 Standard Model Gauge Bosons and
12 Ghosts of Conformal Gravitons (Root Vectors of $U(2,2)$)
that live on the nearest-neighbor links and represent 24 of 600-cell vertices.

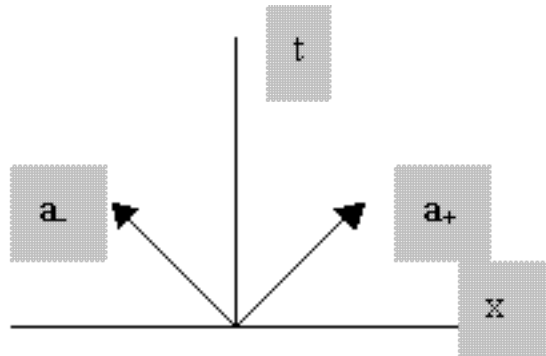
D+4sm vertices have 6-semi-HyperCube 32 next-next-nearest neighbors representing
4 CP2 Internal Symmetry Space components of 8 First-Generation Fermion Particles.
Fermion AntiParticles are represented by Particles moving backward in Time
for representation of $2 \times 32 = 64$ of 600-cell vertices.

D+4g odd (1 and 3) layers correspond to Vectors and Fermion Spinors which are related by Triality.
D+4g even (2) layers correspond to BiVectors.

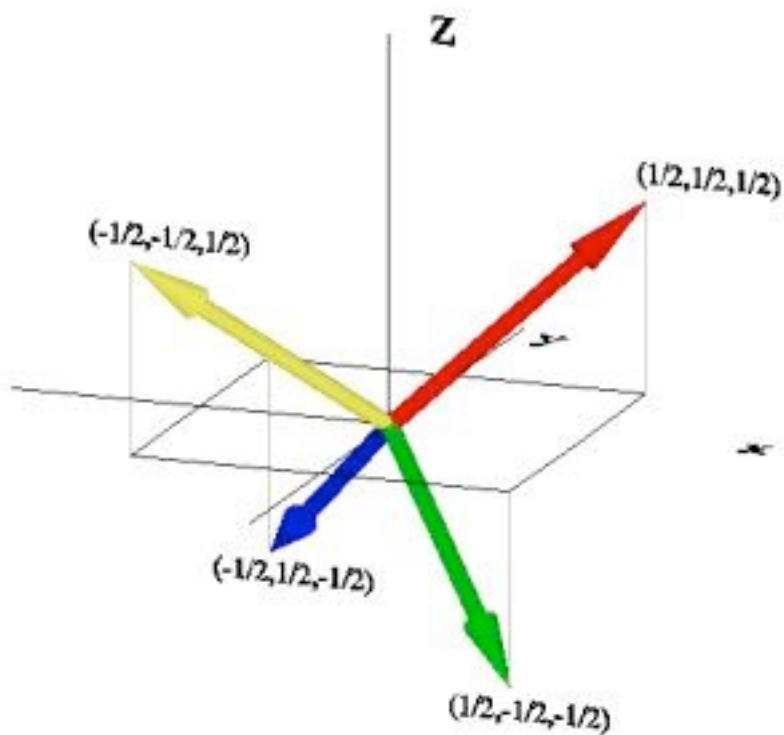
**From each vertex of the 4D Feynman Checkerboard the Second Stage
uses a second Triad of Quantum Choice Vectors.**

**A significant consequence of using two Triads of Quantum Choice Vectors
is the emergence of Second and Third Generation Fermions.**

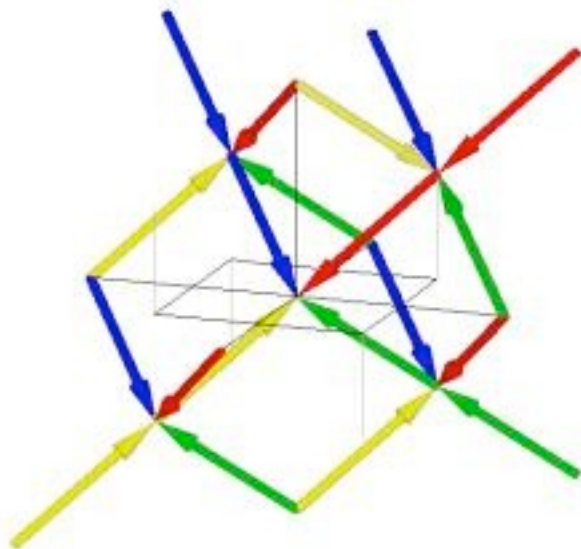
In my earlier paper (arXiv quant-ph/9503015) I used a **simpler version of 4D Feynman Checkerboard which is useful for showing consistency with the Dirac equation** using the following approach: The Feynman Checkerboard in 1+3 SpaceTime dimensions reproduces the Dirac equation, using work of Urs Schreiber and George Raetz. (See my paper at CERN-CDS-EXT-2004-030) A very nice feature of the George Raetz web site is its illustrations, which include an image of a vertex of a 1+1 dimensional Feynman Checkerboard



and an image of a projection into three dimensions of a vertex of a 1+3 dimensional Feynman Checkerboard



and an image of flow contributions to a vertex in a HyperDiamond Random Walk from the four nearest neighbors in its past



Urs Schreiber wrote on the subject:

Re: Physically understanding the Dirac equation and 4D

in the newsgroup sci.physics.research on 2002-04-03 19:44:31 PST (including an appended forwarded copy of an earlier post)
and again on 2002-04-10 19:03:09 PST as found on the web page
<http://www-stud.uni-essen.de/~sb0264/spinors-Dirac-checkerboard.html>

and the following are excerpts from those posts:

"... I know ... the ... lanl paper ... [<http://xxx.lanl.gov/abs/quant-ph/9503015>]...
and

I know that Tony Smith does give
a generalization of Feynman's summing prescription from 1+1 to 1+3 dimensions.

But I have to say that I fail to see that this generalization reproduces the Dirac propagator in 1+3 dimensions,
and that I did not find any proof that it does.

Actually, I seem to have convinced myself that it does not,
but
I may of course be quite wrong.

I therefore take this opportunity to state my understanding of these matters.

First, I very briefly summarize (my understanding of) Tony Smith's construction: The starting point is the observation that the left $|-\rangle$ and right $|+\rangle$ going states of the 1+1 dim checkerboard model can be labeled by complex numbers

$|-\rangle \rightarrow (1 + i)$
 $|+\rangle \rightarrow (1 - i)$

(up to a factor) so that multiplication by the negative imaginary unit swaps components:

$(-i)(1 + i)/2 = (1 - i)/2$
 $(-i)(1 - i)/2 = (1 + i)/2$

Since the path-sum of the 1+1 dim model reads
 $\phi = \text{sum over all possible paths of } (-i \text{ eps } m)^{(\text{number of bends of path})} =$
 $= \text{sum over all possible paths of product over all steps of one path of } -i \text{ eps } m$
 (if change of direction after this step generated by i) 1 (otherwise)
 this makes it look very natural to identify the imaginary unit appearing in the sum over paths with the "generator" of kinks in the path.

To generalize this to higher dimensions, more square roots of -1 are added, which gives the quaternion algebra in 1+3 dimensions.

The two states $|+\rangle$ and $|-\rangle$ from above, which were identified with complex numbers, are now generalized to four states identified with the following quaternions (which can be identified with vectors in M^4 indicating the direction in which a given path is heading at one instant of time):

$$(1 + i + j + k) (1 + i - j - k) (1 - i + j - k) (1 - i - j + k) ,$$

which again constitute a (minimal) left ideal of the algebra

(meaning that applying i,j, or k from the left on any linear combination of these four states gives another linear combination of these four states).

Hence,

now i,j,k are considered as "generators" of kinks in three spatial dimensions and the above summing prescription naturally generalizes to

$$\phi = \text{sum over all possible paths of product over all steps of one path of}$$

$$-i \text{ eps } m \text{ (if change of direction after this step generated by i)}$$

$$-j \text{ eps } m \text{ (if change of direction after this step generated by j)}$$

$$-k \text{ eps } m \text{ (if change of direction after this step generated by k)}$$

$$1 \text{ (otherwise)}$$

The physical amplitude is taken to be

$$A * e^{(i \alpha)}$$

where A is the norm of phi and alpha the angle it makes with the x0 axis.

As I said, this is merely my paraphrase of Tony Smith's proposal as I understand it.

I fully appreciate that the above construction is a nice (very "natural") generalization of the summing prescription of the 1+1 dim checkerboard model.

But if it is to describe real fermions propagating in physical spacetime, this generalized path-sum has to reproduce the propagator obtained from the Dirac equation in 1+3 dimensions, which we know to correctly describe these fermions. Does it do that?

...

Hence I have taken a look at the material [that] ... George Raetz ... present[s] ... titled "The HyperDiamond Random Walk", found at

http://www.pcisys.net/~bestwork.1/QRW/the_flow_quaternions.htm ,

which is mostly new to me. ...

I am posting this in order to make a suggestion for a more radical modification

...

[The]... equation ... $DQ = (iE)Q$... is not covariant.

That is because of that quaternion E sitting on the left of the spinor Q

in the rhs of [the] equation

The Dirac operator D is covariant,

but the unit quaternion E on the rhs refers to a specific frame.

Under a Lorentz transformation L one finds

$L DQ = iE LQ = L E' Q \Leftrightarrow DQ = E'Q$ now with $E' = L^{-1} E L$ instead of E .

This problem disappears

when the unit quaternion E is brought to the *right* of the spinor Q .

What we would want is an equation of the form $DQ = Q(iE)$.

In fact, demanding that the spinor Q be an element of the minimal left ideal generated by the primitive projector $P = (1+y_0)(1+E)/4$,

so that $Q = Q' P$,

one sees that $DQ = Q(iE)$ almost looks like the the *Dirac-Lanczos equation*

(See hep-ph/0112317, equation (5) or ... equation (9.36) [of]... W. Baylis, Clifford (Geometric) Algebras, Birkhaeuser (1996) ...).

To be equivalent to the Dirac-Lanczos equation, and hence to be correct,

we need to require that $D = \gamma_0 @0 + \gamma_1 @1 + \gamma_2 @2 + \gamma_3 @3$

instead of ... = $\gamma_0 @0 + e_1 @1 + e_2 @2 + e_3 @3$.

All this amounts to sorting out

in which particular representation we are actually working here.

In an attempt to address these issues, I now redo the steps presented on

http://www.pcisys.net/~bestwork.1/QRW/the_flow_quaternions.htm

with some suitable modifications to arrive at the correct Dirac-Lanczos equation

(this is supposed to be a suggestion subjected to discussion):

So consider a lattice in Minkowski space

generated by a unit cell spanned by the four (Clifford) vectors

$$\begin{aligned} r &= (\gamma_0 + \gamma_1 + \gamma_2 + \gamma_3)/2 & g &= (\gamma_0 + \gamma_1 - \gamma_2 - \gamma_3)/2 & b &= \\ & & & & &= (\gamma_0 - \gamma_1 + \gamma_2 - \gamma_3)/2 & y &= (\gamma_0 - \gamma_1 - \gamma_2 + \gamma_3)/2 . \end{aligned}$$

(γ_i are the generators of the Dirac algebra $\{\gamma_i, \gamma_j\} = \text{diag}(+1, -1, -1, -1)_{ij}$.)

This is Tony Smith's "hyper diamond".

(Note that I use Clifford vectors instead of quaternions.)

Now consider a "Clifford algebra-weighted" random walk along the edges of this lattice,

which is described by four Clifford valued "amplitudes": K_r, K_g, K_b, K_y and

such that

$$@_r K_r = k (K_g \gamma_2 \gamma_3 + K_b \gamma_3 \gamma_1 + K_y \gamma_1 \gamma_2)$$

$$@_b K_b = k (K_y \gamma_2 \gamma_3 + K_r \gamma_3 \gamma_1 + K_g \gamma_1 \gamma_2) \quad @_g K_g = k (K_r \gamma_2 \gamma_3 + K_y \gamma_3 \gamma_1 + K_b \gamma_1 \gamma_2)$$

$$@_y K_y = k (K_b \gamma_2 \gamma_3 + K_g \gamma_3 \gamma_1 + K_r \gamma_1 \gamma_2) .$$

(This is geometrically motivated. The generators on the rhs are those that rotate the unit vectors corresponding to the amplitudes into each other. "k" is some constant.)

Note that I multiply the amplitudes from the *right* by the generators of rotation, instead of multiplying them from the left.

Next, assume that this coupled system of differential equations is solved by a spinor Q

$$Q = Q' (1+y_0)(1+iE)/4$$

$$E = (y_2 y_3 + y_3 y_1 + y_1 y_2)/\sqrt{3} \text{ with}$$

$$K_r = r Q \quad K_g = g Q \quad K_b = b Q \quad K_y = y Q .$$

This ansatz for solving the above system by means of a single spinor Q is, as I understand it, the central idea.

But note that I have here modified it on the technical side:

Q is explicitly an algebraic Clifford spinor in a definite minimal left ideal,

E squares to -1, not to +1,

and the K_i are obtained from Q by premultiplying with the Clifford basis vectors defined above.

Substituting this ansatz into the above coupled system of differential equations one can form one covariant expression by summing up all four equations:

$$(r @r + g @g + b @b + y @y) Q = k \sqrt{3} Q E$$

The left hand side is immediate.

To see that the right hand side comes out as indicated

simply note that $r + g + b + y = y_0$ and that $Q y_0 = Q$ by construction.

The above equation is the Dirac-Lanzos-Hestenes-Guersey equation, the algebraic version of the equation describing the free relativistic electron.

The left hand side is the flat Dirac operator $r @r + g @g + b @b + y @y = \gamma_m @m$ and

the right hand side, with $k = mc / (\hbar \sqrt{3})$,

is equal to the mass term $i mc / \hbar Q$.

As usual, there are a multitude of ways to rewrite this.

If one wants to emphasize biquaternions then

premultiplying everything with y_0 and

splitting off the projector P on the right of Q to express everything in terms of the,

then also biquaternionic, Q' (compare the definitions given above)

gives Lanzos' version (also used by Baylis and others).

I think this presentation improves a little on that given on George Raetz's web site:

The factor E on the right hand side of the equation is no longer a nuisance but a necessity.

Everything is manifestly covariant (if one recalls that algebraic spinors are manifestly covariant when nothing non-covariant stands on their *left* side). The role of the quaternionic structure is clarified, the construction itself does not depend on it. Also, it is obvious how to generalize to arbitrary dimensions. In fact, one may easily check that for 1+1 dimensions the above scheme reproduces the Feynman model.

While I enjoy this, there is still some scepticism in order as long as a central question remains to be clarified:

How much of the Ansatz $K(r,g,b,y) = (r,g,b,y) Q$ is wishful thinking?

For sure, every Q that solves the system of coupled differential equations that describe the amplitude of the random walk on the hyper diamond lattice also solves the Dirac equation.

But what about the other way round?
Does every Q that solves the Dirac equation also describe such a random walk. ...".

My proposal to answer the question raised by Urs Schreiber
**Does every solution of the Dirac equation
also describe a HyperDiamond Feynman Checkerboard random walk?**
uses symmetry.

The hyperdiamond random walk transformations include the transformations of the Conformal Group:

rotations and boosts (to the accuracy of lattice spacing);
translations (to the accuracy of lattice spacing);
scale dilatations (to the accuracy of lattice spacing): and
special conformal transformations (to the accuracy of lattice spacing).

Therefore, to the accuracy of lattice spacing, the hyperdiamond random walks give you all the conformal group Dirac solutions, and since the full symmetry group of the Dirac equation is the conformal group, the answer to the question is "Yes".

Thanks to the work of Urs Schreiber:
**The HyperDiamond Feynman Checkerboard in 1+3 dimensions does reproduce
the correct Dirac equation.**

Here are some references to the **conformal symmetry of the Dirac equation**:

R. S. Krausshar and John Ryan in their paper Some Conformally Flat Spin Manifolds, Dirac Operators and Automorphic Forms at math.AP/022086 say:

"... In this paper we study Clifford and harmonic analysis on some conformal flat spin manifolds. ... manifolds treated here include RP^n and $S^1 \times S^{(n-1)}$.

Special kinds of Clifford-analytic automorphic forms associated to the different choices of are used to construct Cauchy kernels, Cauchy Integral formulas, Green's kernels and formulas together with Hardy spaces and Plemelj projection operators for L_p spaces of hypersurfaces lying in these manifolds. ...

Solutions to the Dirac equation are called Clifford holomorphic functions or monogenic functions.

Such functions are covariant under ... conformal or Mobius transformations acting over $R^n \cup \{\infty\}$".

Barut and Raczka, in their book Theory of Group Representations and Applications (World 1986), say, in section 21.3.E, at pages 616-617:

"... E. The Dynamical Group Interpretation of Wave Equations.

... Example 1. Let $G = O(4,2)$.

Take U to be the 4-dimensional non-unitary representation in which the generators of G are given in terms of the 16 elements of the algebra of Dirac matrices as in exercise 13.6.4.1.

Because $(1/2)L_{56} = \gamma_0$ has eigenvalues $n = +/-1$,

taking the simplest mass relation $mn = K$, we can write

$(m \gamma_0 - K) \Psi(\dot{p}) = 0$, where K is a fixed constant.

Transforming this equation with the Lorentz transformation of parameter E

$\Psi(p) = \exp(i E N) \Psi(p)$

$N = (1/2) \gamma_0 \gamma_a$

gives

$(\gamma^u p_u - K) \Psi(p) = 0$

which is the Dirac equation ...".

P. A. M. Dirac, in his paper Wave Equations in Conformal Space, Ann. Math. 37 (1936) 429-442, reprinted in The Collected Works of P. A. M. Dirac: Volume 1: 1924-1948, by P. A. M. Dirac (author), Richard Henry Dalitz (editor), Cambridge University Press (1995), at pages 823-836, said:

"... by passing to a four-dimensional conformal space ...

a ... greater symmetry of ... equations of physics ... is shown up, and their invariance under a wider group is demonstrated. ...

The spin wave equation ... seems to be the only

simple conformally invariant wave equation involving the spin matrices. ... This

equation is equivalent to the usual wave equation for the electron, except ...[that it is multiplied by]... the factor $(1 + \alpha_5)$,

which introduces a degeneracy. ...".

Here are some comments on **Lorentz Invariance based on D4 Lattice** properties:

The D4 lattice nearest neighbor vertex figure, the 24-cell,
is the 4HD HyperDiamond lattice next-to-nearest neighbor vertex figure.

Fermions move from vertex to vertex along links.

Gauge bosons are on links between two vertices, and so can also be considered as moving from vertex to vertex along links.

The only way a translation or rotation can be physically defined is by a series of movements of a particle along links.

A TRANSLATION is defined as a series of movements of a particle along links, each of which is

the CONTINUATION of the immediately preceding link IN THE SAME DIRECTION.

An APPROXIMATE rotation, within an APPROXIMATION LEVEL D , is defined with respect to a given origin as a series of movements of a particle along links among vertices ALL of which

are in the SET OF LAYERS LYING WITHIN D of norm (distance²) R from the origin, that is,

the SET OF LAYERS LYING BETWEEN norm $R-D$ and norm $R+D$ from the origin.

Conway and Sloane (Sphere Packings, Lattices, and Groups - Springer) pp. 118-119 and 108, is the reference that I have most used for studying lattices in detail.

(Conway and Sloane define the norm of a vector x to be its squared length xx .)

In the D4 lattice of integral quaternions,

layer 2 has the same number of vertices as layer 1, $N(1) = N(2) = 24$.

Also (this only holds for real, complex, quaternionic, or octonionic lattices),

$K(m) = N(m)/24$ is multiplicative,

meaning that, if p and q are relatively prime, $K(pq) = K(p)K(q)$.

The multiplicative property implies that:

$K(2^a) = K(2) = 1$ (for a greater than 0) and

$K(p^a) = 1 + p + p^2 + \dots + p^a$ (for a greater than or equal to 0).

So,

for the D4 lattice,

there is always an arbitrarily large layer (norm $xx = 2^a$, for some large a)

with exactly 24 vertices, and

there is always an arbitrarily large layer (norm $xx = P$, for some large prime P)

with $24(P+1)$ vertices (note that Mersenne primes are adjacent to powers of 2),

and

given a prime number P whose layer is within D of the origin,

which layer has N vertices,

there is a layer kP with at least N vertices within D of any other given layer in D4.

Some examples I have used are chosen so that

the 2^a layer adjoins the prime $2^a \pm 1$ layer.

The notation in the following table is based on the minimal norm of the D4 Lattice being 1, in which case **the D4 lattice is the lattice of integral quaternions**. This is the second definition (equation 90) of the D4 Lattice in Chapter 4 of Sphere Packings, Lattices, and Groups, 3rd ed., by Conway and Sloane (Springer 1999) who note that the Dn lattice is the checkerboard lattice in n dimensions.

m=norm of layer	N(m)=no. vert.	K(m)=N(m)/24
1	24	1
2	24	1
3	96	4
4	24	1
5	144	6
6	96	4
7	192	8
8	24	1
9	312	13
10	144	6
11	288	12
12	96	4
13	336	14
14	192	8
15	576	24
16	24	1
17	432	18
18	312	13
19	480	20
20	144	6
127	3,072	128
128	24	1
65,536=2 ¹⁶	24	1
65,537	1,572,912	65,538
2,147,483,647	51,539,607,552	2,147,483,648
2,147,483,648=2 ³¹	24	1

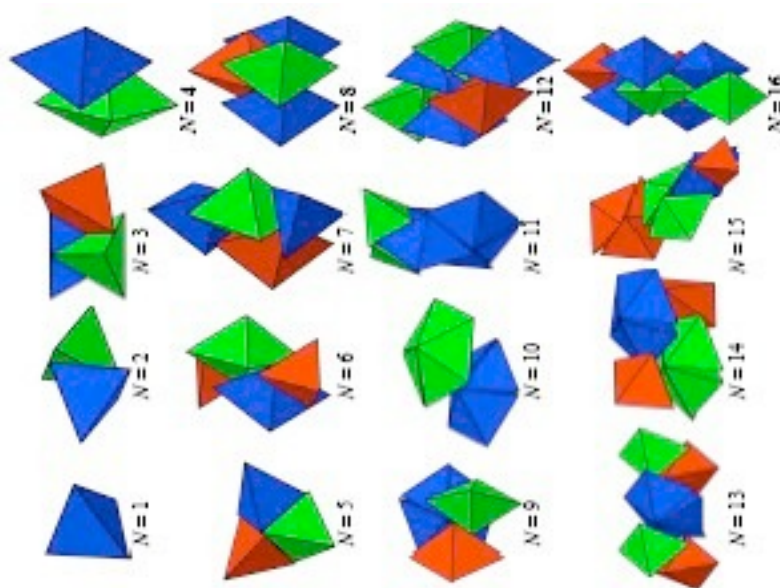
The 57G - 81G Pearce - 600-cell - 240 E8 construction with tetrahedra requires that the initial flat 3-dim space be curved

What happens if you require the 3-dim space to remain flat ?

If you construct with (exactly regular) tetrahedra in 3-dim space that remains flat that is like making a tetrahedral dense packing of flat 3-dim space.

The densest such packing now known is described by Chen, Engel, and Glotzer in arXiv 1001.0586 :

“... We present the densest known packing of regular tetrahedra with density $\Phi = 4000 / 4671 = 0.856347 \dots$



... The dimer structures are remarkable in the relative simplicity of the 4-tetrahedron unit cell as compared to the 82-tetrahedron unit cell of the quasicrystal approximant, whose density is only slightly less than that of the densest dimer packing.

The dodecagonal quasicrystal is the only ordered phase observed to form from random initial configurations of large collections of tetrahedra at moderate densities. It is thus interesting to note that for some certain values of N, when the small systems do not form the dimer lattice packing, they instead prefer clusters (motifs) present in the quasicrystal and its approximant, predominantly pentagonal dipyrramids. This suggests that the two types of packings - the dimer crystal and the quasicrystal/ approximant - may compete, raising interesting questions about the relative stability of the two very different structures at finite pressure. ...”.

If you regard a Tetrahedron as a pair of Binary Dipoles



then the Chen - Engel - Glotzer high (0.85+) density configurations have the same 8-periodicity property as the Real Clifford Algebras:

#Binary Dipoles M	Maximum Density		Success Rate	Motifs, Structural Description
	Numerical, $\hat{\phi}$	Analytical, ϕ		
2	0.367346	18/49	100%	1 monomer [11]
4	0.719486	ϕ_2	100%	2 monomers, transitive [22]
6	0.666665	2/3	21%	3 monomers, three-fold symmetric
8	0.856347	4000/4671	80%	2 dimers (positive + negative)
10	0.748096	ϕ_5	22%	1 pentamer, asymmetric
12	0.764058	ϕ_6	11%	2 dimers + 2 monomers
14	0.749304	3500/4671	15%	2 x 2 dimers minus 1 monomer
16	0.856347	4000/4671	44%	2 x 2 dimers, identical to $N = 4$
18	0.766081		—	1 pentagonal dipyrmaid + 2 dimers
20	0.829282	ϕ_{10}	2%	2 pentagonal dipyrmaids
22	0.794604		—	1 nonamer + 2 monomers
24	0.856347	4000/4671	3%	3 x 2 dimers, identical to $N = 4$
26	0.788728		4%	1 pentagonal dipyrmaid + 4 dimers
28	0.816834		3%	2 pentagonal dipyrmaids + 2 dimers
30	0.788693		—	Disordered, non-optimal
32	0.856342	4000/4671	< 1%	4 x 2 dimers, identical to $N = 4$
⋮	⋮			⋮
164x8	0.850267			Quasicrystal approximant [21]

which is consistent with regarding the 4 vertices of a Tetrahedron as the 4 elements of the Cl(2) Real Clifford Algebra, isomorphic to the Quaternions, with graded structure 1+2+1, and so 4 tetrahedra as Cl(4x2) = Cl(8).

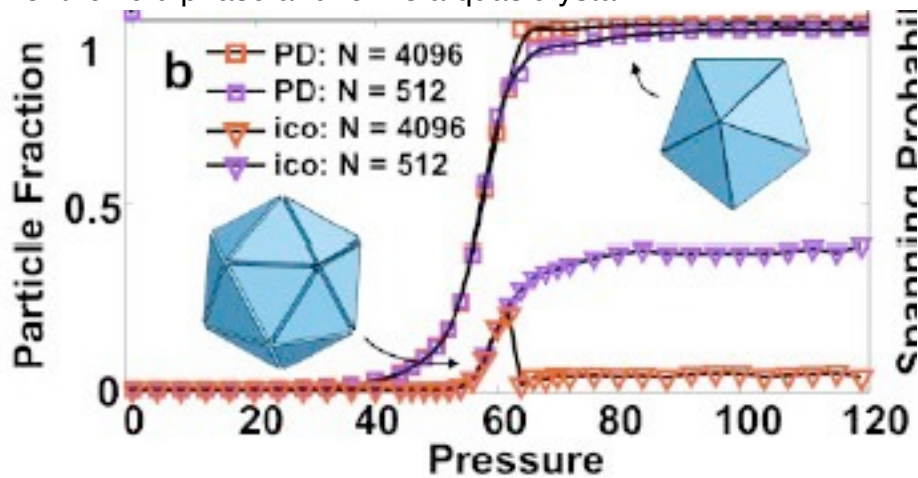
The Large N Limit of 4N Tetra Clusters =
 = **Completion of Union of All 4N Tetra Clusters** would correspond to
 the same generalized Hyperfinite II₁ von Neumann factor of Cl(16)-E8 Physics
 that gives a natural Algebraic Quantum Field Theory structure.

What about the QuasiCrystal / approximant in flat 3-dim space ?

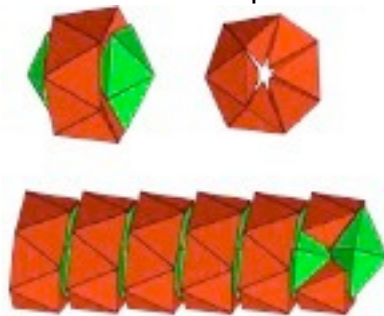
Haji-Akbari¹, Engel, Keys, Zheng, Petschek, Palffy-Muhoray, and Glotzer in arXiv 1012.5138 say: "... a fluid of hard tetrahedra undergoes a first-order phase transition to a dodecagonal quasicrystal, which can be compressed to a packing fraction of $\phi = 0.8324$. By compressing a crystalline approximant of the quasicrystal, the highest packing fraction we obtain is $\phi = 0.8503$.

...

To obtain dense packings of hard regular tetrahedra, we carry out Monte-Carlo (MC) simulations ... of a small system with 512 tetrahedra and a large system with 4096 tetrahedra. ... The large system undergoes a first order transition on compression of the fluid phase and forms a quasicrystal. ...



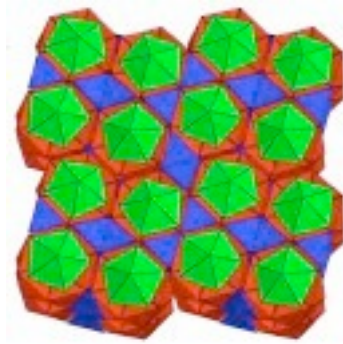
... the quasicrystal consists of a periodic stack of corrugated layers ... Recurring motifs are rings of twelve tetrahedra that are stacked periodically to form "logs"...



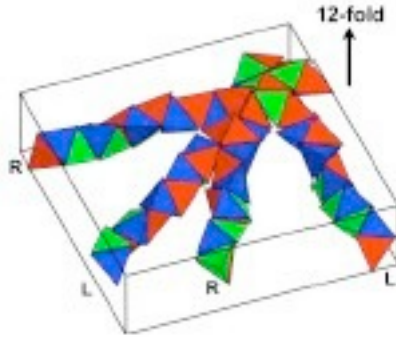
... Perfect quasicrystals are aperiodic while extending to infinity; they therefore cannot be realized in experiments or simulations, which are, by necessity, finite. ...

Quasicrystal approximants are periodic crystals with local tiling structure identical to that in the quasicrystal. Since they are closely related, and they are often observed in experiments, we consider them as candidates for dense packings.

The dodecagonal approximant with the smallest unit cell (space group) has 82 tetrahedra ...



... At each vertex we see the logs of twelve-member rings (shown in red) capped by single PDs (green). The logs pack well into squares and triangles with additional, intermediary tetrahedra (blue). The vertex configuration of the tiling is ...



...”

The QuasiCrystal approximant is not as dense as the 4N Tetra Cluster packing, so I do not regard it as being as useful for fundamental physics as the 4N Tetra packing.

The true QuasiCrystal is less dense than the QuasiCrystal approximant, so I regard it as being less useful for fundamental physics. However, as Sadoc and Mosseri say in their book “Geometrical Frustration” (Cambridge 2005) “... quasiperiodic structures [can be] derived from the eight-dimensional lattice E8. ... using the cut and project method, it is possible to generate a four-dimensional quasicrystal having the symmetry of the [600-cell] polytope {3,3,5} ... a shell-by-shell analysis ...

Table A9.1. Number of vertices on shells surrounding the origin in the E8 lattice. The first shell is a Gosset polytope in eight dimensions

N	Squared radius r^2	Vertices on E8 shell
1	1/2	240
2	1	2160
3	3/2	6720

... recalls in some respects ... the Fibonacci chain ...

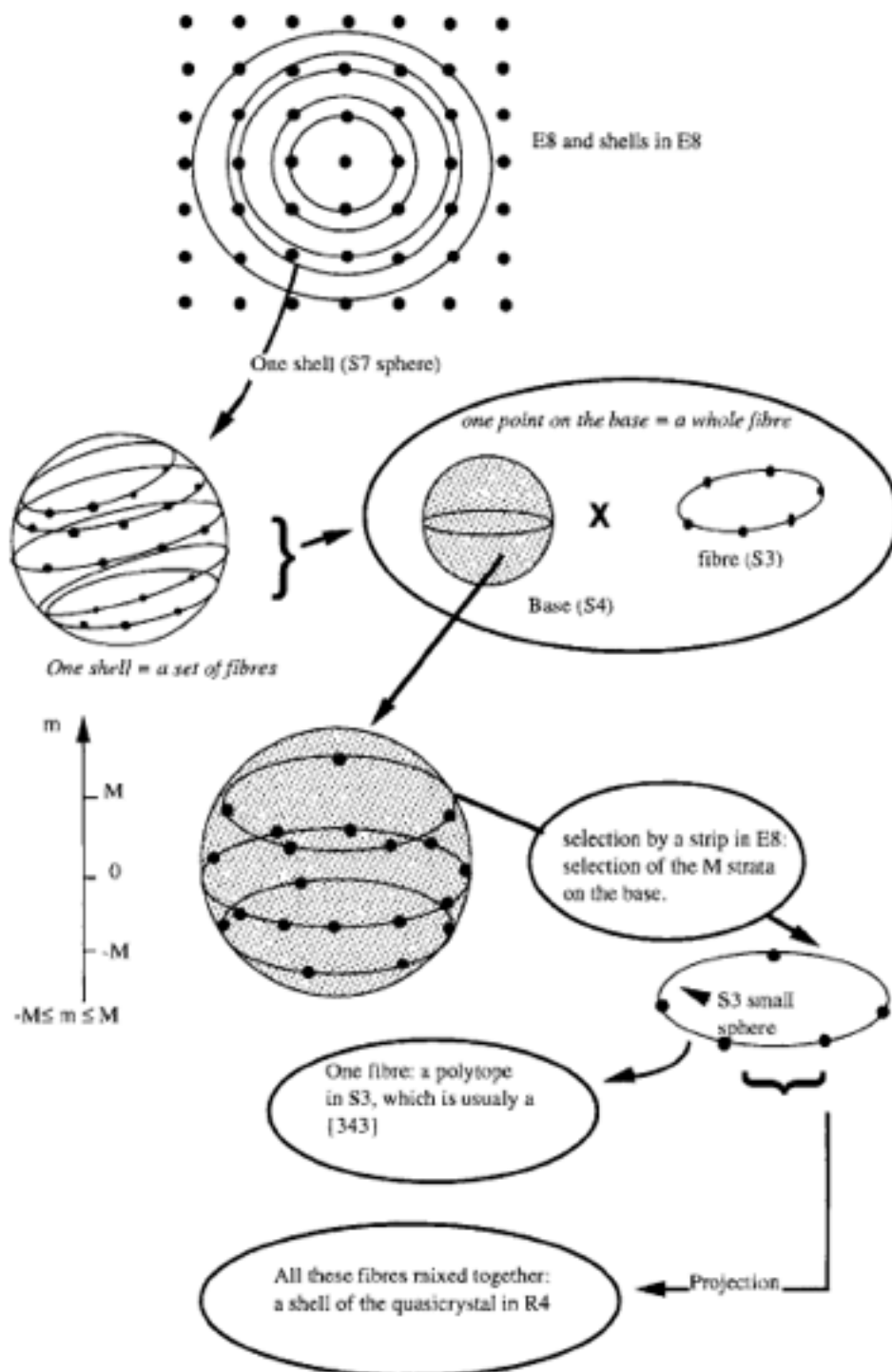


Fig. A9.1. Scheme summarizing the four-dimensional construction method: take an E_8 shell, considered as a discrete fibration of S^7 , select the fibres which map (H-map) onto a stratum M of the base of the fibration, and finally orthogonally map (O-map) the selected sites onto R^4 .

The relationship between QuasiCrystals and QuasiCrystal approximants is discussed by An Pang Tsai in an IOP review “Icosahedral clusters, icosahedral order and stability of quasicrystals - a view of metallurgy”:

“... we overview the stability of quasicrystals ... in relation to phason disorder ... the phonon variable leads to long wavelength and low energy distortion of crystals, the phason variable in quasicrystals leads to a ... type of distortion ... Let a two-dimensional lattice points sit at the corners of squares in a grid. ... a strip with a slope of an irrational number ... golden mean ... is ... a Fibonacci sequence and is exactly a one-dimensional quasicrystal ... [if] the slope of the strip is ... a rational number ... [it]... is a periodic sequence ... [and]... is called an approximant ... in the approximant where the sequence changes by a flip ... This flip is called phason flip ... a flipping of tiles in two-dimensions or three-dimensions ...

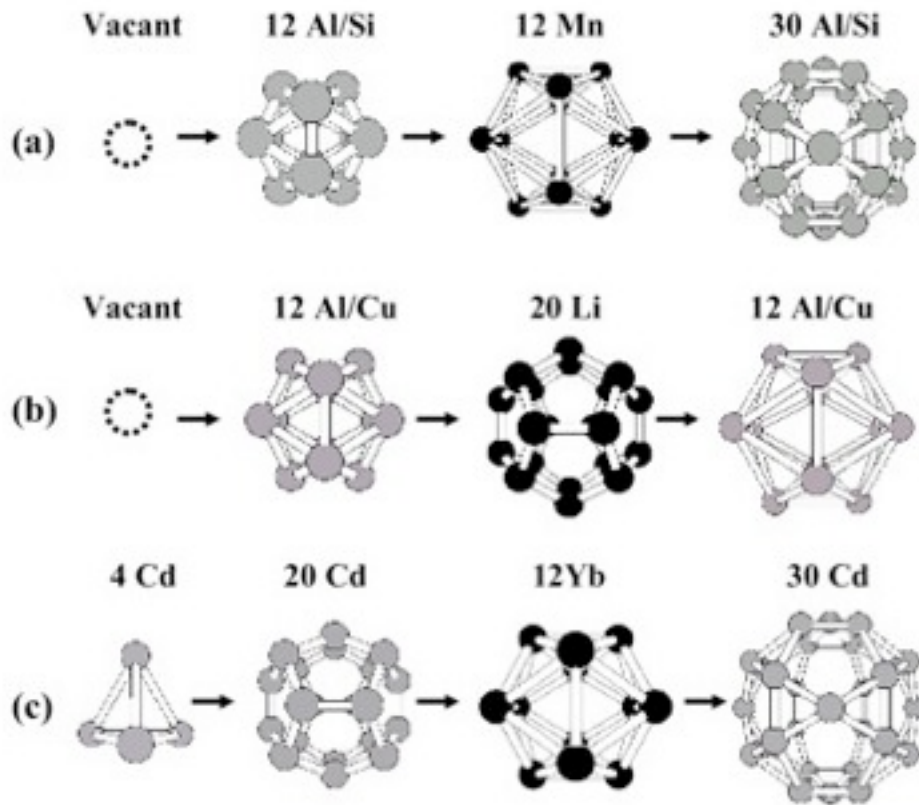


Figure 3. Concentric structures of three types of icosahedral clusters derived from three $1/1$ approximants of quasicrystals. (a) The Al-Mn-Si class or Mackay icosahedral cluster: the center is vacant, the 1st shell is an Al/Si icosahedron, the 2nd shell is a Mn icosahedron, and the 3rd shell is an Al/Si icosidodecahedron. (b) The Zn-Mg-Al class or Bergman cluster: an example is R-Al₁₃Cu; the center is vacant, the 1st shell is an Al/Cu icosahedron, the 2nd shell is a Li dodecahedron, the 3rd shell is a larger Al/Cu icosahedron. (c) The Cd-Yb class: the center is a Cd tetrahedron, the 1st shell is a Cd dodecahedron, the 2nd shell is a Yb icosahedron, and the 3rd shell is a Cd icosidodecahedron.

... ‘phason strain’ ... is the characteristic disorder for quasicrystals but does not exist in crystals ... a fully annealed stable iQc [icosahedral quasicrystal]... is almost free of phason disorder ...”.